

Energy Efficient Battery Management

Carla F. Chiasserini
Dipartimento di Elettronica
Politecnico di Torino
Torino, Italy
chiasserini@polito.it

Ramesh R. Rao
Dept. of Electrical and Computer Engineering
University of California, San Diego
La Jolla, CA, USA
rrao@ucsd.edu

Abstract—A challenging aspect of mobile communications consists in exploring ways in which the available run time of the terminals can be maximized. In this paper we investigate battery management techniques that can dramatically improve the energy efficiency of radio communication devices. We consider an array of electrochemical *cells* connected in parallel. Through simple scheduling algorithms the discharge from each cell is properly shaped to optimize the charge recovery mechanism, without introducing any additional delay in supplying the required power. Then, a traffic management scheme, that exploits the knowledge of the cells state of charge, is implemented to achieve a further improvement in the battery performances. In this case, the discharge demand may be delayed. Results indicate that the proposed battery management techniques improve system performance no matter which parameters values are chosen to characterize the cells behavior.

I. INTRODUCTION

As the popularity of radio communications equipments increases, the reliability and energy capacity of batteries becomes a critical issue. Indeed, a greater battery capacity means a longer run time of the terminals, and therefore it is a determining factor in the success of a product. Due to the disparity in the rate of technological advance in batteries and in portable communications equipments markets, software/hardware solutions have to be found to improve the battery performance.

As shown by experimental tests [1], [2], [3] and analytical results [4], [5], a greater battery capacity can be obtained by using a pulsed current discharge instead of a constant current discharge. In fact, under a pulsed discharge profile the charge recovery mechanism inherent to many secondary storage batteries can be exploited. During the interruptions of the drained current, so called *rest time periods*, the battery is able to recover charge thanks to the *diffusion process* [4]. Longer rest times translate into a greater capacity delivered by the battery [6]. An application of the pulsed discharge technique and its benefits can be observed in GSM and other TDMA based systems, where a high current is needed from the battery just during the packet transmission time (e.g., $557 \mu\text{s}$ in GSM), otherwise a value of current about 10 times lower is drained [7]. For a summary of the behavior of real batteries, please refer to [4].

In this paper, we explore ways in which the energy efficiency of mobile wireless communications can be enhanced through the use of improved energy-efficient battery management tech-

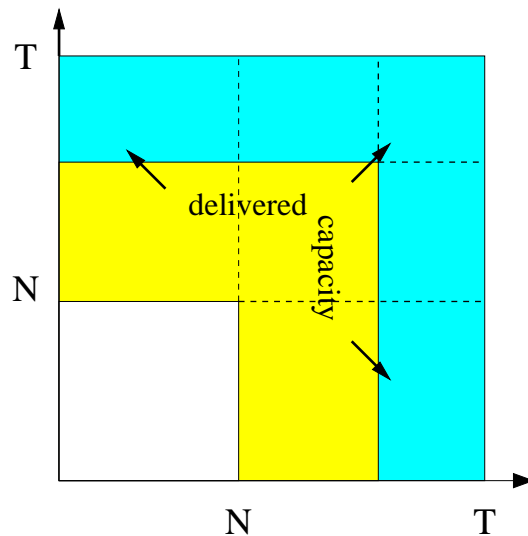


Fig. 1. Margin of improvement for the capacity delivered by an array of $L=2$ cells.

niques. We consider a battery package of L cells¹ that can be selectively scheduled. Concerns about the increase of the portable equipment size due to the implementation of the cells array, may be solved by considering lithium-polymer cells [8], [9]. These cells can be shaped as needed and even made as flat as a credit card. Examples of systems that switch between different battery cells already exist, but at times such cells are not connected in parallel since they are used to switch between different values of voltage [10].

Let us denote the initial charge of a cell by N , and its maximum amount of available capacity by T . Fig. 1 illustrates the case for $L=2$. A capacity equal to N can be drained from each cell by means of a constant current discharge. However, by using a proper pulsed discharge technique, the region of delivered capacity can be increased. Our goal is to find methods to extend the region of delivered capacity up to the maximum limit. Indeed, in the presence of bursty data traffic, we may be able to adjust traffic arrivals and battery discharge profile so that the recovery mechanism can be fully exploited.

We apply simple scheduling techniques to efficiently dis-

Supported by NSF under grant CCR 9714651.
Carla F. Chiasserini is on leave at the University of California, San Diego.

¹A cell is the basic electrochemical device; a battery can be composed of one or more than one cells connected in series and/or in parallel.

tribute the discharge demand among the cells. In the *delay-free* approach the power supply is provided as soon as required. By using the battery model presented in [5], we show that a significant improvement in battery capacity is achieved. When scheduling algorithms are used in conjunction with traffic shaping, the battery is always able to deliver its maximum available capacity even for high traffic arrival rates. In this case the price to pay is a small additional delay. This approach is named *no-delay-free*.

The discharge policies proposed may not be the optimal since our objective here is to show that energy efficiency can be enhanced by exploiting battery characteristics in innovative ways. In any case, the search for optimality must also be balanced against the need to accurately model batteries and to keep the overall system as simple as possible.

The remainder of the paper is organized as follows: Sect. II describes the delay-free battery management techniques; Sect. III introduces the postulated cell model, presents the analysis carried out to derive the battery performance when delay-free schemes are implemented, and shows some results; Sect. IV illustrates the proposed no-delay-free technique and obtained improvements; finally, Sect. V concludes the paper.

II. DELAY-FREE BATTERY MANAGEMENT TECHNIQUES

We consider that the battery package is composed of an array of L cells. The battery discharge demand is driven by Poisson distributed traffic arrivals. We assume a discrete time system with time slot length equal to 1 and we define a *job arrival* as the event that one or more packets arrive in a time slot. Thus, considering a Poisson process with rate R , at each time slot the probability that i packets arrive is

$$a_i = \frac{R^i e^{-R}}{i!} \quad i \geq 0. \quad (1)$$

Denoting the job inter-arrival time by τ , the probability that the inter-arrival time is equal to k time slots is geometrically distributed

$$P\{\tau = k\} = e^{-R(k-1)}(1 - e^{-R}). \quad (2)$$

The usual method to drain power from cells connected in parallel is to draw off the same amount of current from all the cells whenever a power supply is required. Thus, we consider that as soon as a job arrives, all the L cells are discharged for a time duration equal to one slot and the drained current for each packet is equal to $1/L$ the required supply. Note that the packet arrival process at each cell is Poisson with rate R and the distribution of the inter-arrival time is as in (2). We refer to this scheme as the joint technique (JN).

Here, we apply to the cells array two different scheduling techniques and we compare their performances with those derived by using the JN method. We point out that both the following scheduling algorithms are independent of the cells state of charge and assume that at each job arrival the time necessary

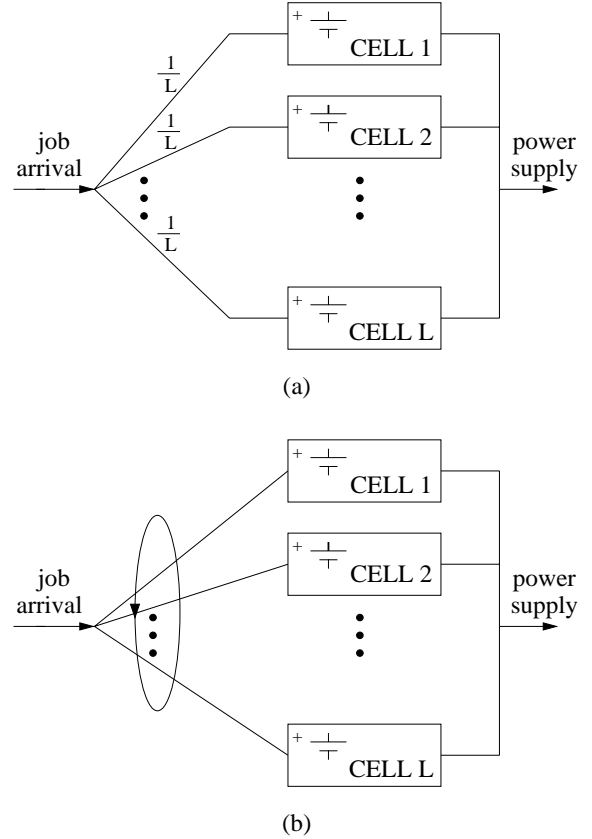


Fig. 2. Scheduling algorithms applied to the cells discharge: (a) random (RD); (b) round robin (RR).

to drain the required current supply is always equal to one time slot.

The first technique that we consider is a random scheme, indicated by RD, such that a job arrival is directed to each of the L cells with probability equal to $1/L$, regardless of the number of packets constituting the job. The packet arrival process at each cell is still Poisson but with rate equal to R/L . A graphical representation of the RD scheme is given in the upper picture of Fig. 2.

The second technique is the round robin scheduling shown in the lower picture of Fig. 2. The job arrivals are directed to the cells by switching from a cell to the next one. In this case, the distribution of the job inter-arrival times is derived by convolving L probability functions, whose expression is written in (2). For $L = 2$, we have

$$P\{\tau = k\} = (k-1)e^{-R(k-2)}(1 - e^{-R})^2. \quad (3)$$

III. DELAY-FREE APPROACH PERFORMANCE

In order to derive the battery performance when the scheduling algorithms described in the previous section are applied to the discharge process, we adopt the cell model presented in [5]. Here, we just give a succinct description of the model to let the reader understand the following analysis; more details can be found in [5].

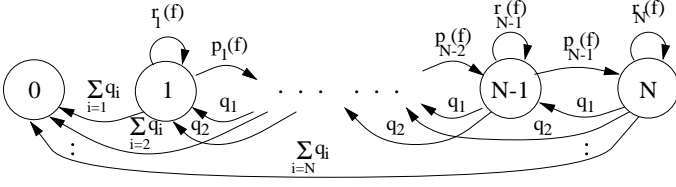


Fig. 3. Stochastic process representing the cell behavior.

A. The Cell Model

The transient model, shown in Fig. 3, tracks the stochastic evolution of a single cell from the fully charged state (N) to the completely discharged state (0). Discharges occur at stochastic instants determined by the discharge pattern and recovery may occur whenever there is no discharge. Each fully charged cell is assumed to have an initial charge equal to N charge units and a maximum available capacity equal to T charge units. The amount of capacity necessary to transmit a packet is considered equal to c_p charge units.

Let us define q_i to be the probability that i charge units are required in one time slot, i.e., the probability that i/c_p packets arrive. During the discharge process, different phases can be identified according to the recovery capability of the cell. Each phase f ($f=0, \dots, f_{max}$) starts right after d_f charge units have been drained from the cell and ends when the amount of discharged capacity reaches d_{f+1} charge units. The probability of recovering one charge unit in a time slot, conditioned on being in state j and phase f is

$$p_j(f) = \begin{cases} a_0 e^{-g_N(N-j) - g_C(f)} & j=1, \dots, N-1 \\ & f=0 \\ a_0 e^{-g_N(N-j) - g_C(f)d_f} & j=1, \dots, N-1 \\ & f=1, \dots, f_{max} \end{cases} \quad (4)$$

where g_N and g_C are parameters that depend on the recovery capability of the battery. In particular, a small value of g_N represents a high cell conductivity, while a large g_N corresponds to a high internal resistance, i.e., a steep discharge curve for the cell. The value of g_C is related to the cell voltage drop during the discharge process, and therefore, to the discharge current. We assume that g_N is a constant, whereas g_C is a piecewise constant function of the number of charge units already drawn off the cell, that changes value in correspondence with d_f ($f=1, \dots, f_{max}$).

We have $d_0=0$ and $d_{f_{max}+1} = T$, while for d_f ($f=1, \dots, f_{max}$) and the corresponding g_C proper values are chosen in order to match the discharge of the cell to experimental results. The values taken by these parameters greatly vary depending on the considered battery technology as well as the current level drawn off the cell.

The probability to remain in the same state of charge while

being in phase f is

$$r_j(f) = a_0 - p_j(f) \quad j=1, \dots, N-1 \quad (5)$$

$$r_N(f) = a_0. \quad (6)$$

It is worth mentioning that a good agreement was found between the results predicted by the postulated stochastic model and those obtained from a numerical code that solves the partial differential equations that model the underlying fine-grained electrochemical phenomenon. This code was developed independently by Newman and others in the Department of Chemical Engineering at UC Berkeley. The program was modified to let the discharge of the cell be driven by a stochastic process representing the data packets generation [11].

B. Performance Analysis

The time period between the end of a job transmission and the arrival of the next job at the cell is the cell rest time. When an arrival occurs, the required charge units are drained in a time slot duration. We define the cell rest time and the following time slot, where the arrival takes place, as a *cycle time*. Then, we model the discharge process of the single cell by considering just the time instants corresponding to the end of cycle times.

In each of the discharge phases the transition probabilities $p_l(f)$ and $r_l(f)$ ($l=1, \dots, N$; $f=0, \dots, f_{max}$) are constant values, thus we start our analysis dealing with the four phases separately. We denote by $v_{i,j}^l(f)$ the probability to move from state l to state $l-i$ in a cycle time, consuming $j c_p$ charge units, and conditioned at being in phase f . Similarly, $w_j^l(f)$ is defined as the probability to remain in the same state l , and $z_{i,j}^l(f)$ as the probability to move to state $l+i$. Since each packet transmission implies the consumption of c_p charge units, i.e., c_p backward steps in the chain shown in Fig. 3, while each recovered charge unit corresponds to one forward step, we can write for $l=1, \dots, N-1$

$$v_{i,j}^l(f) = P \{ \text{arrival of } j \text{ packets} \cdot P \{ \text{recovery} = j c_p - i \mid l, f \} \} \quad (7)$$

$$w_j^l(f) = P \{ \text{arrival of } j \text{ packets} \cdot P \{ \text{recovery} = j c_p \mid l, f \} \} \quad (8)$$

$$z_{i,j}^l(f) = P \{ \text{arrival of } j \text{ packets} \cdot P \{ \text{recovery} = j c_p + i \mid l, f \} \} \quad (9)$$

where

$$P \{ \text{arrival of } j \text{ packets} \} = a_j. \quad (10)$$

Since the cell state of charge cannot exceed N , starting from state l a cell can recover $N-l$ charge units at most in a rest time period. The probability to recover m ($0 \leq m \leq N-l$) charge units during a rest time period can be easily derived looking at Fig. 3,

$$P \{ \text{recovery} = 0 \mid l, f \} = \sum_{k=0}^{\infty} P \{ \tau = k+1 \} r_l^k \quad (11)$$

$$P\{\text{recovery} = m > 0 \mid l, f\} = \sum_{k=m}^{\infty} P\{\tau = k + 1\} \\ [p_l(f) \cdots p_{l+m-1}(f)] [r_l(f) + \dots + r_{l+m}(f)]^{k-m}. \quad (12)$$

For instance, in the case of Poisson traffic and $m > 0$, by substituting (2) in (12), we have

$$P\{\text{recovery} = m \mid l, f\} = (1 - e^{-R})e^{-Rm} \cdot \frac{[p_l(f) \cdots p_{l+m-1}(f)]}{\{1 - e^{-R} [r_l(f) + \dots + r_{l+m}(f)]\}}. \quad (13)$$

Let us define $u_{l,e}^{(f)}(h, n)$ as the probability to reach state e ($0 \leq e \leq N$) starting from state l ($1 \leq l \leq N$) in n cycle times, consuming h charge units, and conditioned at being in the phase of discharge f . For $n = 1$ and $h \geq 1$, we can write

$$u_{N,e}^{(f)}(h, 1) = \begin{cases} \sum_{j=\lceil \frac{h}{c_p} \rceil}^{\infty} a_j & \text{for } e = 0 \text{ and } h = N \\ a_{\frac{h}{c_p}} & \text{for } e > 0 \text{ and } h = N - e \end{cases} \quad (14)$$

$$u_{l,e}^{(f)}(h, 1) = \begin{cases} P\{\text{recovery} = h - l \mid l, f\} \cdot \sum_{j=\lceil \frac{h}{c_p} \rceil}^{\infty} a_j & \text{for } e = 0 \\ v_{l-e, \frac{h}{c_p}}^l(f) & \text{for } 0 < e < l \\ w_{\frac{h}{c_p}}^l(f) & \text{for } e = l \\ z_{e-l, \frac{h}{c_p}}^l(f) & \text{for } e > l \end{cases} \quad 1 \leq l < N. \quad (15)$$

For $n > 1$, two different cases have to be considered. If the number of charge units consumed during phase f is less than or equal to $(d_{f+1} - d_f)$, the process will still be in phase f at the end of n cycle times. Instead, if the amount of charge units drained while being in phase f is greater than $(d_{f+1} - d_f)$, the process will enter phase $f + 1$ at the end of the n -th cycle.

The evolution of the process for $n > 1$ and h such that the process is still in phase f at the end of n cycle times is given by the following equations

$$u_{N,e}^{(f)}(h, n) = \sum_{j=1}^{\lfloor \frac{h}{c_p} \rfloor} \sum_{i=1}^{\min(jc_p, N-1)} a_j u_{N-i,e}^{(f)}(h - jc_p, n - 1) \quad (16)$$

$$u_{l,e}^{(f)}(h, n) = \sum_{j=1}^{\lfloor \frac{h}{c_p} \rfloor} \sum_{i=1}^{\min(jc_p, l-1)} v_{i,j}^l(f) u_{l-i,e}^{(f)}(h - jc_p, n - 1) +$$

$$\sum_{j=1}^{\lfloor \frac{h}{c_p} \rfloor} w_j^l(f) u_{l,e}^{(f)}(h - jc_p, n - 1) +$$

$$\sum_{j=1}^{\lfloor \frac{h}{c_p} \rfloor} \sum_{i=1}^{N-l} z_{i,j}^l(f) u_{l+i,e}^{(f)}(h - jc_p, n - 1) \quad 1 < l < N \quad (17)$$

$$u_{1,e}^{(f)}(h, n) = \sum_{j=1}^{\lfloor \frac{h}{c_p} \rfloor} w_j^1(f) u_{1,e}^{(f)}(h - jc_p, n - 1) + \sum_{j=1}^{\lfloor \frac{h}{c_p} \rfloor} \sum_{i=1}^{N-1} z_{i,j}^1(f) u_{1+i,e}^{(f)}(h - jc_p, n - 1). \quad (18)$$

Eqs. (16)-(18) can be solved iteratively for each possible value of h and n ($n \leq (d_{f+1} - d_f)/c_p$) with the boundary conditions

$$u_{l,e}^{(f)}(h, n) = 0 \quad \text{for } n > 1, h < c_p \text{ and } \forall l, e. \quad (19)$$

The probability that the discharge process passes from phase f to phase $f + 1$ at the end of n cycle times and having consumed h charge units, is equal to the probability to drain $k < h$ charge units in $n - 1$ cycle times without leaving phase f , multiplied by the probability to spend $h - k$ charge units during the last cycle time. Clearly, this can be easily computed once we solve (14)-(18).

At this point, we can derive the average number of charge units, A_{cu} , drained from a cell during the discharge process. For the sake of simplicity let us consider just two phases of discharge ($f=0, 1$). Three different events may occur: (i) the discharge process ends in the state 0 after n cycle times while being in phase $f = 0$ and having consumed h ($h \leq T$) charge units; (ii) the discharge process ends in the state 0 after n cycle times while being in phase $f = 1$ and having consumed h ($h \leq T$) charge units; (iii) T charge units are consumed after n cycle times without having the process reached state 0.

Since the cell is assumed to be in phase 0 and state N at the beginning of the discharge process, the probabilities of the three events are

$$P\{(i) \mid h, n\} = \begin{cases} u_{N,0}^{(0)}(h, n) & \text{if } h \leq d_1 \text{ or } n = 1 \\ \sum_{k=1}^{d_1-1} \sum_{s=1}^N u_{N,s}^{(0)}(k, n - 1) & \text{if } h > d_1 \text{ and } n > 1 \end{cases} \quad (20)$$

$$P\{(ii) \mid h, n\} = \sum_{m=1}^N \sum_{t=1}^N [u_{N,t}^{(0)}(d_1, m) u_{t,0}^{(1)}(h - d_1, n - m) +$$

$$\sum_{s=1}^N \sum_{k=d_1}^{h-1} \sum_{j=1}^{d_1-1} u_{N,s}^{(0)}(j, m-1) u_{s,t}^{(0)}(k-j, 1) \cdot u_{t,0}^{(1)}(h-k, n-m) \quad (21)$$

$$P\{(iii) | n\} = \sum_{e=1}^N \left\{ \sum_{s=1}^N \sum_{k=1}^{d_1-1} u_{N,s}^{(0)}(k, n-1) u_{s,e}^{(0)}(T-k, 1) + \sum_m \sum_{t=1}^N \left[u_{N,t}^{(0)}(d_1, m) u_{t,e}^{(1)}(T-d_1, n-m) + \sum_{s=1}^N \sum_{k=d_1}^{T-1} \sum_{j=1}^{d_1-1} u_{N,s}^{(0)}(j, m-1) u_{s,t}^{(0)}(k-j, 1) \cdot u_{t,e}^{(1)}(T-k, n-m) \right] \right\}. \quad (22)$$

Thus, we have

$$A_{cu} = \sum_n \left(\sum_{h=1}^T h \cdot P\{(i) | h, n\} + \sum_{h=d_1+1}^T h \cdot P\{(ii) | h, n\} + T \cdot P\{(iii) | n\} \right). \quad (23)$$

The mean number of packets actually transmitted, A_p , results as the ratio of the total average number of charge units drained from the array of cells to the number of charge units consumed per packet,

$$A_p = L \cdot A_{cu} / c_p. \quad (24)$$

If we consider as a performance index the ratio of A_p to the maximum number of packets that can be transmitted by the cells array, we have

$$G = (A_p \cdot c_p) / (T \cdot L) = A_{cu} / T. \quad (25)$$

Therefore, knowing A_{cu} is sufficient to derive the system performance, and, once we characterize the arrival process at each cell, we can just analyze the behavior of the single cell.

C. Results

The behavior of the performance index G is derived for delay-free schemes as a function of the average packet arrival rate R . We assume $T=200$, $c_p=L=2$, and $f_{max} = 3$. While the value assumed for f_{max} is based on experimental results [12], the value taken for T is much smaller than the maximum available capacity in real cells. This choice is due to the complexity in solving the analytical model for greater values of T ; however, simulations run for more realistic values of T qualitatively give the same performance.

Fig. 4 shows results for $N=25$ and g_N varying. Clearly, both the round robin (RR) and the random (RD) algorithms outperform the joint (JN) scheme. This is due to the fact that, in the

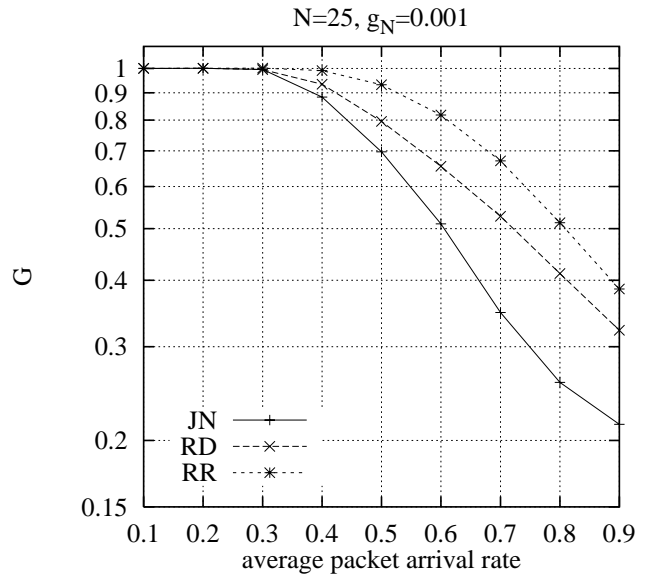
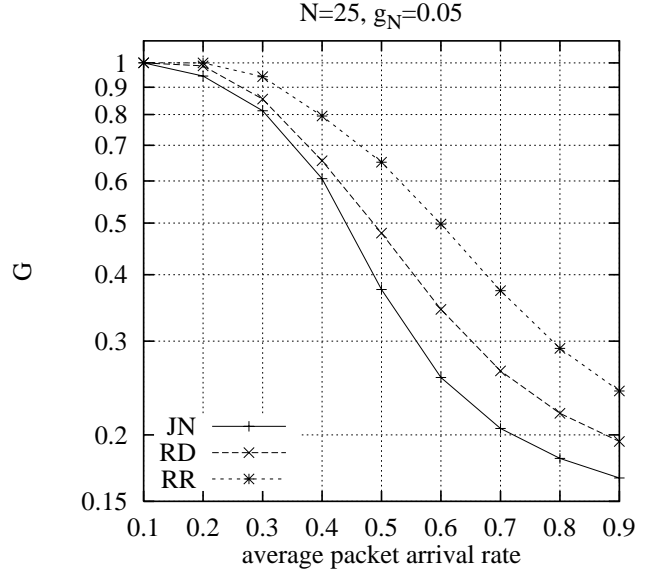


Fig. 4. Gain obtained applying different discharge techniques for $N=25$, $T=200$, and g_N varying. CJ=joint discharge; RD=random; RR=round robin.

case of the RR and RD schemes, the cell rest time period is longer. Thus, even if the current drained per packet from each cell doubles, the chance to recover becomes greater, in particular for high values of the mean packet arrival rate. Moreover, since the rest time duration under the RR technique is always twice that experienced under the JN method, round robin is the best scheme. Finally, for all the considered cases the gain that we obtain increases as g_N decreases, i.e., as the charge recovery capability of the cells improve.

Fig. 5 shows similar results for $N=50$. Here, the initial charge of the cells is larger, therefore the number of charge units the cells are able to deliver is higher. Notice that in the

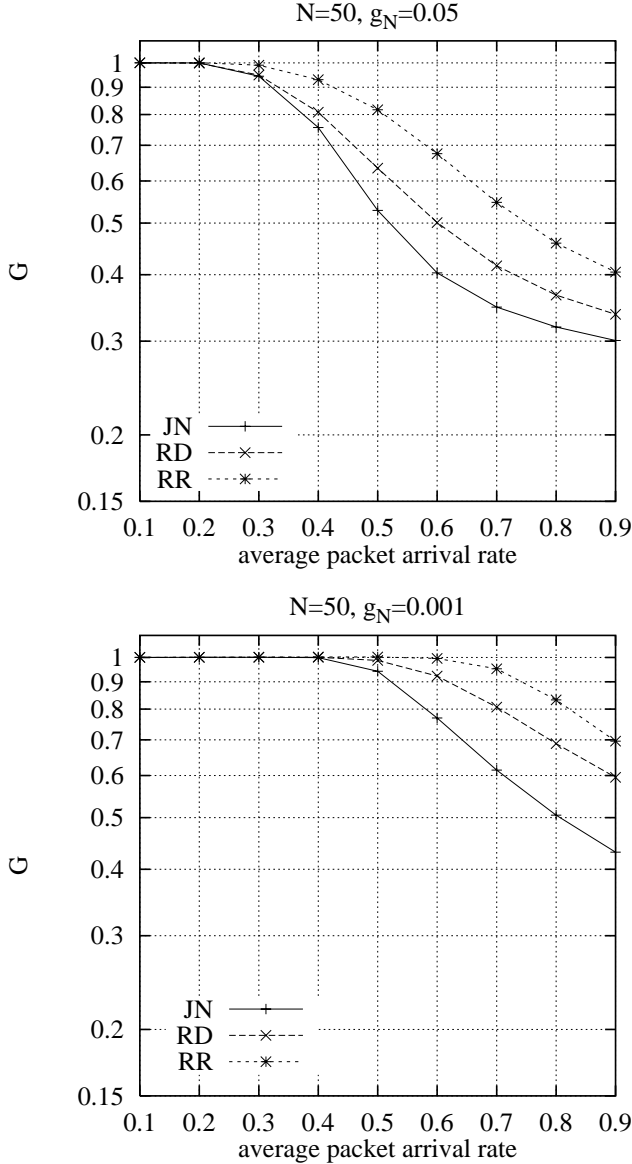


Fig. 5. Gain obtained applying different discharge techniques for $N=50$, $T=200$, and g_N varying. CJ=joint discharge; RD=random; RR=round robin.

case of the RR scheme and $g_N=0.001$, the delivered capacity approaches the maximum that can be obtained for almost any value of the average packet arrival rate.

We conclude that an efficient way to discharge a battery is to guarantee to each cell a rest time long enough to recover. A relevant performance improvement is achieved by adopting a simple round robin technique and this improvement is evident no matter which values for the cells parameters are considered. The performance of a modified RR algorithm, that operates taking into account the cell state of charge in the job assignment to the cells, has been derived by simulation. However, no significant differences have been noted in the behavior of G

with respect to the results presented here for the RR method.

IV. A NO-DELAY-FREE APPROACH

In this section, we consider a battery management technique that involves a coordination among the cells of the array and drains current from the cells according to their state of charge.

Thanks to smart battery packages [13], it is possible to track the discharged capacity of the cells. Our goal is to monitor the cells status and make them recover as much as they need to obtain the maximum available capacity from the discharge process.

We define a lower threshold for the cell state of charge such that whenever the state of charge drops to this value, the cell is considered *not active* and current cannot be drawn off until recovery occurs. The event of the cell state of charge dropping to a certain threshold can be easily revealed by the control apparatus present in smart battery packages; the acquisition of the information is therefore considered instantaneous.

Among the set of active cells, a round robin scheme is applied as described in Sect. II. Whenever the state of charge of a cell drops to the value of threshold, the cell is removed from the set of active cells and allowed to recover. If none of the cells is active, the packets that arrive are buffered and transmitted as soon as a sufficient amount of charge is recovered. We also assume that if a cell becomes not active while serving a packet, the remaining necessary charge is drained from the next active cell.

During the last phase of the discharge process the above scheme is suspended and cells are just discharged as much as we can since at this point recovery becomes quite unlikely.

In this scheme, an important parameter for the cell behavior is the difference between the initial value of charge, N , and the charge threshold that is chosen. We denote this quantity by M . Of course, for a given threshold higher N is, larger M can be taken.

Results obtained by simulation are presented in Figs. 6–9 for $c_p=L=2$ and $f_{max}=3$. We derive the mean packet delay conditioned to being actually transmitted, and the throughput, computed as the ratio of the number of transmitted packets to the discharge process duration. Note that here the performance index G , previously considered, is always equal to 1, that is its maximum value.

In Figs. 6 and 7 plots are obtained for $T=200$, $g_N=0.05$, and M varying. For any value of M , as the mean packet arrival rate grows, the average delay increases. In fact, in this case to let the cells recover properly, the delay introduced between the arrival of a job and the time instant of its transmission becomes greater. However, for small values of M better performances are obtained, especially for high values of the packet arrival rate. Note also that when a large M is considered, the throughput decreases as the arrival rate increases. This is because, as soon as the discharge process starts, the cell quickly reaches the value of threshold, that is far away from the initial charge. At this point, the recovery probability is low and the time to

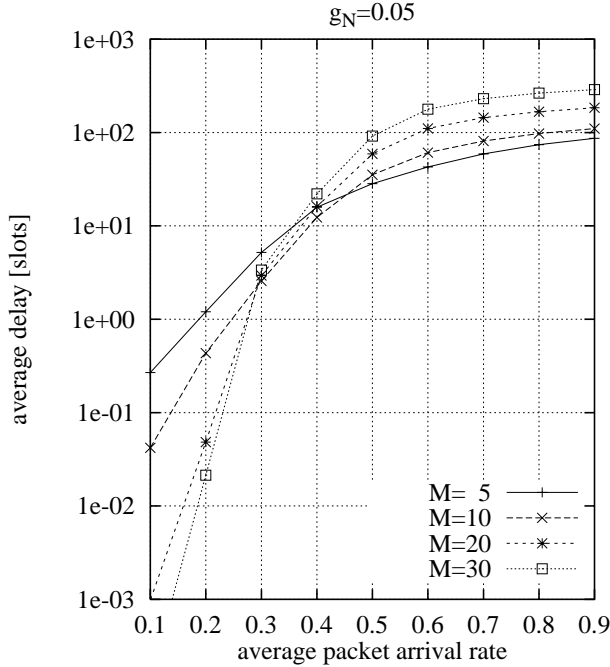


Fig. 6. Average packet delay introduced when the proposed no-delay-free technique is implemented. $T=200$, $g_N=0.05$, and M varying.

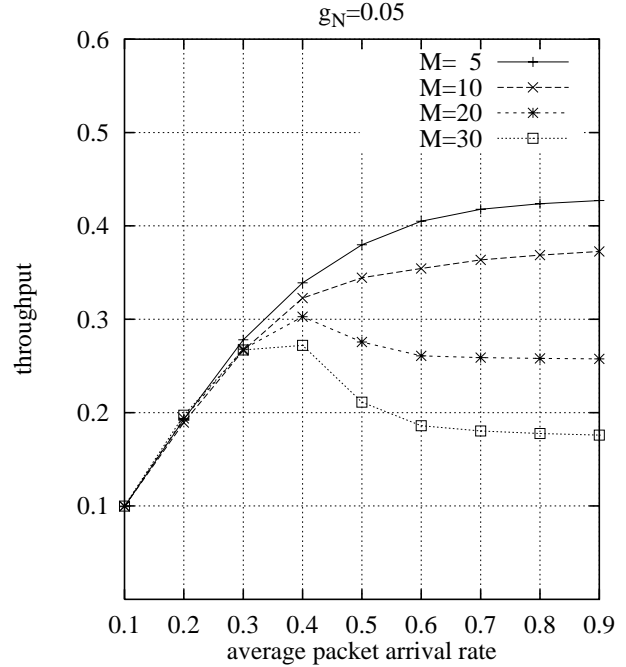


Fig. 7. Throughput obtained using the proposed no-delay-free technique. $T=200$, $g_N=0.05$, and M varying.

wait before being able to resume the packet transmission becomes large; thus, the time period needed to drain from the cell the total number of available charge units increases. When this effect takes place, we have to reduce the cell load by using a larger array of cells so that we move to a more favorable region of operation.

In Figs. 8 and 9, the curves are presented for $T=200$ and $g_N=0.001$. Now, the recovery capability of the cells is much superior, thus, the achieved throughput is higher and the average delay is far below 100 time slots even for an average packet arrival rate equal to 0.9. Larger values of M give better performances since now cells are able to quickly recover even when their state of charge is greatly reduced relative to the initial value.

We highlight that implementing the proposed battery management technique, a significant gain in performances is obtained and this can be achieved with a reasonably small additional delay in the packet transmission for any value of the cell parameters. The improvement with respect to a simple round robin scheme is evident; however, in this case a smart battery package has to be used and a greater complexity is required.

V. CONCLUSIONS

In this paper, we explored battery management techniques to improve the battery capacity, and therefore the run time of communications devices. A battery package composed of an array of cells was considered. The combination of the charge recovery mechanism with traffic management techniques ap-

plied to the cells array showed an increase in the battery performance. Improvement was observed regardless of the values assumed for the parameters characterizing the cell behavior.

Analytical results indicated that performance can be significantly increased without introducing any delay in the packet transmission by implementing a round robin scheme. Moreover, it was shown by simulation that a battery is able to deliver the maximum available capacity at the expense of a fairly small additional delay and complexity when a round robin scheduling is combined with a simple traffic management technique.

Further work should address the problem of optimality for battery management techniques. The goal is to find the scheme that gives the most efficient battery discharge performance without significant additional cost and complexity.

REFERENCES

- [1] T.F. Fuller, M. Doyle, and J.S. Newman, "Relaxation phenomena in lithium-ion-insertion cells," *J. Electrochem. Soc.*, vol. 141, pp. 982–990, April 1994.
- [2] R.M. LaFollette, "Design and performance of high specific power, pulsed discharge, bipolar lead acid batteries," *10th Annual Battery Conf. on Applications and Advances*, Long Beach, pp. 43–47, January 1995.
- [3] B. Nelson, R. Rinehart, and S. Varley, "Ultrafast pulse discharge and recharge capabilities of thin-metal film battery technology," *11th IEEE Int. Pulsed Power Conf.*, Baltimore, pp. 636–641, June 1997.
- [4] C.F. Chiasserini and R.R. Rao, "Pulsed battery discharge in communication devices," *MobiCom'99*, Seattle, pp. 88–95, August 1999.
- [5] C.F. Chiasserini and R.R. Rao, "A traffic control scheme to optimize the battery pulsed discharge," *Milcom'99*, Atlantic City, November 1999.
- [6] H.D. Linden, *Handbook of batteries*, 2nd ed. New York: McGraw-Hill, 1995.

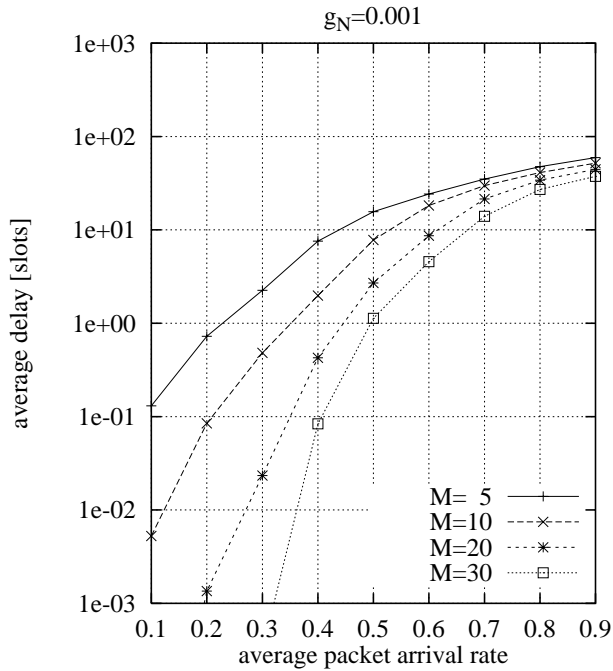


Fig. 8. Average packet delay introduced when the proposed no-delay-free technique is implemented. $T=200$, $g_N=0.001$, and M varying.

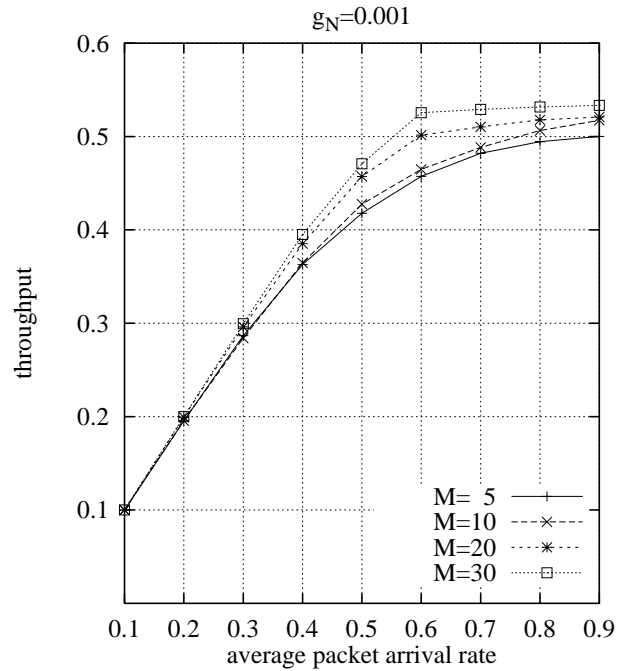


Fig. 9. Throughput obtained using the proposed no-delay-free technique. $T=200$, $g_N=0.001$, and M varying.

- [7] Tadiran Electronic Industries, "Make the right battery choice for portables," <http://www.tadiranbat.com/howrchg.htm>.
- [8] J.W. Halley and B. Nielsen, "Simulation studies of polymer electrolytes for battery applications," *MRS Symposium Proceedings*, vol. 496, pp. 101–107, December 1997.
- [9] H.S. Choe and K.M. Abraham, "Synthesis and characterization of LiNiO_2 as a cathode material for pulse power batteries," *MRS Symposium Proceedings*, vol. 496, pp. 303–308, December 1997.
- [10] Maxim Integrated Products, "Energy management for small portable systems," <http://www.maxim-ic.com>.
- [11] C.F. Chiasserini, R.R. Rao, "Stochastic battery discharge in portable communication devices," *15th Annual Battery Conf. on Applications and Advances*, Long Beach, January 2000.
- [12] J. Broadhead and T. Skotheim, "A safe, fast-charge, two volt lithium/polymer cathode 'AA'-size cell with a greater than 250 Wh kg^{-1} energy density," *J. of Power Sources*, vol. 65, pp. 213–18, 1997.
- [13] Cadex Electronics Inc., "Intelligent batteries," <http://www.cadex.com/cfm/index>.